Ultrastructure changes induced by the phloroglucinol derivative Agrimol G isolated from *Leucosidea sericea* in *Haemonchus contortus*

M. Adamu[1,2], L. Mukandiwa[1,3], M.D. Awouafack[1,4], A.S. Ahmed[1], J.N. Eloff[1], V. Naidoo[1,3]

[1]Department of Paraclinical Sciences, Faculty of Veterinary Science, University of Pretoria, South Africa

[2]Permanent Address: Department of Veterinary Parasitology and Entomology, College of Veterinary Medicine, University of Agriculture, Makurdi, Nigeria

[3]Biomedical Research Centre, Faculty of Veterinary Science, University of Pretoria, South Africa

[4] Permanent Address: Department of Chemistry Universite de Dschang Cameroon

Corresponding Author

Vinny Naidoo: vinny.naidoo@up.ac.za Private Bag X04, Faculty of Veterinary Science, University of Pretoria, Onderstepoort, 0110

Key word: Agrimol; Electron microscopy; Haemonchus; *Leucosidea sericea*; anthelmintic

Highlights

- Agrimol G was isolated from Leucosidea sericea.
- Agrimol resulted in the formation of non-membranous multi-vesicular like bodies.
- The effect of Agrimol was mitigated in the presence of ivermectin or albendazole.
- Agrimol G is concluded to inhibit microtubular polymerisation.

Abstract

Plant extracts used for the treatment of helminth infections in sheep are an alternative to chemical anthelmintic drugs. Previous studies have reported the anthelmintic activity of acetone leaf extracts of *Leucosidea sericea*. For this study, we evaluate the ultrastructure changes induced by the acetone leaf extract of *L. sericea* and the component agrimol G (AG) that was isolated for the first time on adult haemonchus parasites. Adult haemonchus parasites harvested from sheep were incubated with the plant extract and AG for 3 hours and evaluated by both scanning and transmission electron microscopy in comparison and in combination with albendazole or ivermectin. In all cases the method of evaluation shows ultrastructural changes, with albendazaole inducing mitochondrial damage and ivermectin inducing muscle degeneration, both as previously described. Incubation with the plant extract and AG resulted in the formation of numerous non-membrane bound multi-vesicular like bodies and evenly spread disruptions/erosion in the epicuticle. Combining AG with ivermectin or albendazole resulted in an absence of effect of AG. Based on the structural changes induced by AG, together with the absence of an effect in combination with ivermectin and albendazole would suggest a disrupted microtubular network. The latter does however require biochemical confirmation.

Introduction

Through years of use of the anthelminthic drugs, haemonchus has developed severe resistance to all the major class available, threatening sheep farming in certain areas of the world. With newer treatment agents needed, some have suggested that plant based remedies may be a viable alternative (Githiori et al., 2004; Hoste et al., 2006; Adamu et al., 2013). Phytochemical also offers the benefit of having lower environmental impact due to their biodegrabable nature (Waller, 2004, Hoste et al., 2006).

Leucosidea sericea Eckl. & Zeyh (Watt and Breyer-Brandwijk, 1962; Pooley, 1993) is a member of the Rosaceae family, consisting of approximately 3000 species with nine species only indigenous to South Africa. It is a 7 m tall tree of great character, and grows in the eastern parts of South Africa (Coates-Palgrave, 2002). Leaves of this plant is used mainly for anthelmintic purpose, while the Zulu people use a paste made from it for treating opthalmia (Hutchings, 1996). The *in vitro* anthelmintic activity of this species has been reported by Aremu et al (2010) with a minimal lethal concentration of 0.26 mg/ml against *Caenorhabditis elegans*, while Adamu et al (2013) reported a 50% effective concentration of 1.27 ± 0.07 mg/ml in a *Haemonchus contortus* larval development assay. At present the active component and mechanism of action of *L. sericea* is yet to be elucidated.

While the anthelmintics have different mechanisms of action (Köhler, 2001), they tend to function generally within two broad categories. The first being parasitic paralysis and expulsion due to an inability of the parasite to maintain its position within the gastrointestinal tract against peristalsis, while the second is the interference with energy production and subsequent parasite starvation and lysis. Other mechanism of effect are however possible, as evident with the benzimidazole febantel (Mehlhorn and Harder, 1997), where disappearance

of the microtubules of the axons are described (Zintz and Frank, 1982). Further studies have indicated that the benzimidazole compounds bind to the tubulin prior to polymerisation thereby preventing subunit binding into a microtubule (Köhler, 2001). With the microtubules being involved with numerous cellular processes, their destruction leads to death of the organism. For this study we discuss the isolation of agrimol G (AG) as the active component extract, as well as to discuss the ultrastructures changes induced on electron microscopy as a first step in establishing the mechanism of action of the phloroglucinol derivatives as a potential new class of anthelmintic drug.

Material and Methods

Plant material, bulk extraction, fractionation and isolation of compounds

The leaves of *L. sericea* were collected from the National Botanical Garden in Pretoria, South Africa (Voucher number PRU 288). Ground material (500g) was extracted using acetone (10 ml/g) with intermittent shaking for 24 h. For the isolation, the dried acetone extract was subjected to solvent-solvent fractionation to fractionate the crude acetone leaf extract into hexane, chloroform, ethyl acetate and n-butanol fractions based on polarity (Eloff, 1998a). From superior activity, the hexane fraction (3g) was subjected to silica gel open column chromatography (2.5 diameter x 73 cm, 0.0630.200 nm, 100g) using hexane with increasing amount of ethyl acetate to yield 99 fractions of 500 ml each that were combined to 15 fractions after monitoring with comparative TLC. TLC silica gel 60 F_{254} (Merck, Germany) chromatograms were used for monitoring fractions and spots were detected with UV light (254 and 365 nm) and then sprayed with vanillin-sulphuric acid spray reagent followed by heating at 110 ^{o}C for c. 3 min. The best efficacy of the four different fractions and AG was determined using the egg hatch assay (EHA) and the larval development test (LDT) as previously described

by Adamu et al (2013)(results not shown), prior to mechanistic studies on adult worms. IR spectra were recorded on a Bruker Alpha FT-IR spectrometer (Optik GmbH, Germany). ^{1} H- and 13C-NMR spectrum was recorded with a Bruker spectrometer at 500 MHz, and chemical shifts (δ) are quoted in ppm with TMS as internal standard. The structures of the AG isolated compounds was identified by interpretation of their NMR and IR data and by comparison with reported data.

Mechanistic studies on adult parasites

Adult *H. contortus* parasites were obtained from the abomasum of naturally infected sheep at slaughter from a commercial abattoir. The abomasum was tied up from both ends and washed into a bucket, and the motile adult parasite removed by manual hand picking with the help of a needle and parasite identity was confirmed. Parasites (n=36), 1900 µL in PBS, were placed into tubes and incubated for 3 h at 20 °C in an incubator with the 100 µL extract of *L. sericea* (final concentration 1200 µg/ml)(n=10), AG (final concentration at 1200 µg/ml in PBS), albendazole (final concentration 380 µg/ml in PBS) or ivermectin (final concentration 500 µg/ml in PBS) as the positive controls and PBS as the negative control. All the parasites were subsequently subjected to transmission electron microscopy evaluation (TEM) and scanning electron microscopy (SEM).To determine the least effective concentration, parasites were incubated with a final concentration of AG (n=36) at 1200, 600, 300, and 150 µg/ml in PBS and subjected to SEM. In all cases, at minimum 5 adults parasites were evaluated. For the highest concentration of AG, the exposures were undertaken on two separate occasions to ensure consistency in effect.

Mechanism of parasite entry

To further understand the effect of AG, its effect at 1200 µg/mL (n=27) was re-evaluated in

combination with albendazole (380µg/ml) or ivermectin (500µg/ml) by TEM. After incubation, the parasites were washed three times in PBS and then transferred into 2% glutaraldehyde solution for further processing. The rationale behind the co-incubation was two-fold, firstly to see if the second drug had a synergist effect with the AG, and secondly to see how they influenced the activity of AG. Albendazole was selected as it selectively induces dissolution of the microtubules by preventing polymerisation. Ivermectin was selected as stabilises the microtubular network and prevents its damage (Ashraf et al, 2015).

Transmission Electron Microscopy

Samples for electron microscopy were fixed in 2.5 % glutaraldehyde. Thereafter, the fixative was carefully decanted into appropriate waste bottles by means of a pipette. After post-fixation in osmium tetroxide for 1 hour, the tissue blocks were rinsed in Millonigs buffer for 10 min, distilled water for a further 20 min. Thereafter, the specimens were dehydrated using a graded series of ethanol (50%, 70%, 80%, 96%, and 100%) for 10 min each. The sections were then infiltrated with Mollifex twice for 10 min and propylene oxide twice for 10 min each. The sections were then infiltrated with propylene: Epoxy resin mixture at a ratio of 2:1 for 30 min to 1 hour, and then embedded in a 100% epoxy resin overnight. The specimens were cured in embedding oven at 65^0C overnight. Polymerised resin blocks were now ready for ultramicrotomy. Ultra-thin resin sections were contrasted with uranyl acetate and lead citrate before being examined in a Philips CM10 transmission electron microscope operated at 80 kV.

Scanning Electron Microscopy

Samples for electron microscopy were fixed in 2.5 % glutaraldehyde. Thereafter, the fixative was carefully decanted into appropriate waste bottles by means of a pipette. After post-

fixation in osmium tetroxide for 1 hour, the tissue blocks were rinsed in Millonigs buffer for 10 min, distilled water for a further 20 min. Thereafter, the specimens were dehydrated using a graded series of ethanol (50%, 70%, 80%, 96%, and 100%) for 10 min each. The ethanol was discarded and replaced with equal volume of HMDS in a fume cupboard. Specimens were incubated for 30 minutes at room temperature and then resuspended in a small volume of HMDS. A drop of this suspension was placed on a coverslip and air dried. After drying the specimen were coated with gold and viewed at different magnifications (x130, x900, x1800, x4300) using a Zeiss scanning electron microscope.

Interpretation of the EM results

The changes elicited within the parasites and on the parasite surface were compared to published electron micrographs. Specific organelles evaluated were the mitochondria for signs of swelling and loss of internal cristae (Rothwell and Sanger 2006), the accumulation of secretory granules, presence of lysis, and for signs of discontinuation/damage of the cuticle. For granules there were divided into type 1 and II based on their density or lucency as described by Gonçlaves et al (2013).

Results

Three compounds were isolated for the study. They were previously identified *β*-sitosterol (Nair et al, 2012) and newly isolated of agrimol A and agrimol G (Figure 1)(Infrared data for the agrimols are presented in the supplementary information). With *β*-sitosterol being previously shown to have anti-inflammatory and cholesterol reducing activity, it was not evaluated further (Gerson et al, 1964; Nair et al, 2012). Initial studies with both the agrimol compounds showed similar effects (results not shown). With agrimol G isolated in larger quantities, it was evaluated further as below.

Following exposure of adult *H. contortus* parasites to an acetone leaf extract of *Leucosidea sericea*, albendazole, AG, Ivermectin and PBS control, several different ultra-structural internal changes were evident for some of the treatment groups on SEM following 3 hours of incubation (Figure 2). The AG treated parasites consistently showed major external surface disruption that was characterised by distorted circular and longitudinal annulations. The AG treated parasites also appeared to be shrunken, which would be indicative of loss of internal content. In contrast, no damage was evident for albendazole and the saline control, while ivermectin showed very slight changes. When evaluated for the lowest effective dose (Figure 3), the 1200 and 600 µg/ml concentration of AG showed the equivalent effect of generalise cuticular damage, while the lower concentration had only a more localised effect with irregular patches of damage to the cuticle being evident. As a result, the minimal effective concentration of AG appears to be 600 µg/ml.

The various changes evident on TEM are presented in Figure 4. On TEM the saline treated parasites presented with the expected architecture of a layered cuticle covered by a dense epicuticle, absence of vacuolation and numerous mitochondria (approximately 1x2µM). Also present were secretory granules, mainly electron dense which we characterised as Type-1 granules as per previous descriptions. In comparison, various abnormalities of increased vacuolation and changes in the shape of the mitochondria which were larger (1x3 µM) and more irregular were evident for albendazole. For ivermectin, the muscle layers under the integument showed poorly visible myofibrils. All the AG treated parasites showed the presence of a variable number of multi-vesicular like bodies (2 to 2.5 µM), which was not surrounded by a membrane in all the exposed parasites. Around these multi-vesicular like bodies, a large number of electron-dense and electron-lucent bodies of various sizes were

present. Despite these changes, the mitochondria in the AG treated groups appeared to be normal. At the surface of the parasite, AG induced changes to the epicuticle which can best be described as erosions, and were equidistant (1 µM) to each other (Figure 5).

When AG was co-incubated with either ivermectin or albendazole (Figure 6), none of the changes seen with AG alone were present. Nonetheless for albendazole the typical signs of mitochondrial swelling were present (Ho et al.,1994). No obvious changes were evident for the ivermectin co-incubation group.

Discussion

This is the first report of AG, a phloroglucinol derivative, being present in *L sericea*. Aspidin and desaspidin with their structures suggesting that they're likely metabolites of agrimol, were however previously isolated from *L sericea* isolated by Bosman et al. (2004). All the agrimol compounds (A to G) have previously been isolated, especially agrimol B from *Agrimonia pilosa* Ledeb (Wang et al, 2016). The pharmacokinetics of agrimol B has also been evaluated in Sprague Dawley rats (Wang et al, 2016). Following oral gavage, agrimol B was poorly absorbed with a fraction of absorption of 16.4–18.0%. The drug was also characterised by a Tmax of 2.0–2.5 h and a half-life of elimination of 1.7 to 4 hours. While speculative, the latter may be due to a combination of the large size of the molecule that would result in poor cellular permeability of the compound via the intestinal barrier, and the molecule's more lipid solubility of the molecule evident by its isolation in the ethyl acetate fraction. This is also the first report of anthelmintic activity of AG. Despite extensive literature review, no other described biological activity for the molecule could be found. However, the phloroglucinol derivatives as a group have been described to have anthelmintic, antibacterial, antimalarial and antidiabetic activity together with the ability to interfere with

adipocyte differentiation (Lounasmaa et al, 1973; Yamaki et al, 1989; Singh and Bharate, 2006; Wang et al, 2015). Aspidin and desaspidin (Lounasmaa et al., 1973) have also specifically been shown to be effective against tapeworms, with desaspidin being tentatively linked to the inhibition of oxidative phosphorylation as with the niclosamide (Airaksinen et al., 1967).

The main objective of this study was to explore the ultrastructure changes induced by a *L. sericea* acetone extract and one of its components, AG, against adult *H. contortus*. For this we harvested adult parasites from sheep at slaughter. While the resistance status of the parasites was unknown, based on the history of drug helminth resistance reported in South Africa, the strains in question are likely multi-resistant strains (Van Wyk et al., 1999). An incubation period of 3 hours was selected based on the use of the same time period by Brunet et al. (2011) who evaluated efficacy with immature stages and by Gonclaves et al (2013) who evaluated the effects of closantel after 180 minutes of treating Guinea pigs. While this method was previously used by Jasmer et al (2000) to evaluate drug transport, this is the first that we are aware of that its' been successfully applied in evaluating drug activity in the adult parasite. Previous studies relying on the treatment of infected animals and subsequent harvest of grown adults following slaughter or alternately exposing immatures grown under laboratory conditions (Brunet et al, 2011).

The method we've used offers several advantages over the use of immature stages as it targets the intended adult life stage during therapy, it's much easier to facilitate than growing the immatures to adults under *in vitro* conditions and is more ethically sound as sampling is opportunistic at slaughter. The method also provides reliable results during the short incubation period, with the control samples showing no incidence of abnormalities while both

aldendazole and ivermectin showing the expected pathological changes. For ivermectin this was evident as severe degeneration of the sub-cuticular muscle layer, as previously described in ticks treated with ivermectin due to loss of myofibrils albeit much sooner for an unexpected reason for haemonchus (Montasser and Amin, 2010). Likewise, the expected changes of mitochondrial damage and vacuolation were evident for albendazole (Cristina et al, 2014).

Following the exposure of the adult parasite to *L. sericea* or AG very specific bodies, which were best described as non-membrane bound multi-vesciular bodies were evident in the AG treated parasite. Despite numerous literature searches this is the first description of such a structure being evident in any healthy nematode parasite or following anthelmintic exposure. An important distinguishing characteristic of these bodies from traditional multi-vesicular bodies present in mammalian cells was the prominent absence of surrounding membranes. In the mammalian cells, these rare bodies are a form of endosomes that contain membrane-bound vesicles, which can be filled with lysosomes or serve as excretory bodies. While it may be argued that the AG was interfering with excretory functionality of the parasite, with resultant accumulation of excretory bodies through coalescence, we do not believe this to be the case due to the absence of a boundary membrane. In previous studies on the axonemes of the actinophryrid heliozoan, Patterson et al (1982), described similar structures which they called non-membrane bound morulated bodies. They further ascribed the presence of these structures to degeneration changes of the microtubular network from poor fixation of the parasite in addition to arguing against them being excretory bodies since they were not membrane bound. To further demonstrate that these structures were degenerating microtubules, they subsequently incubated the heliozoan under cold conditions or concurrently with colchicine. The rationale was that these conditions were

known to inhibit microtubular polymerisation with the result that they are no longer visible on electron microscopy as they break down into their principle components which are dissolved in the cytoplasm. Following this process, none of the samples subsequently showed the presence of morulated bodies, leading to the conclusion that the structures had to be degenerating microtubules. Hausmann et al (1983) were also able to show the absence of degenerative changes to the microtubular network by taking advantage of the opposite effect, which was to stabilise the microtubular network with taxol so that they were no longer degenerative.

Further support for the multi-vesicular-like bodies being remnants of a degenerative microtubular network, are evident from co-incubation of AG with albendazole or ivermectin. From previous studies, albendazole decreases microtubule polymerization as with colchicine. More importantly, the effects of the benzimidazole have been shown to be higher specific to the helminth microtubular network (Köhler, 2001). Following this co-incubation, no multi-vesicular bodies were present, while the albendazole expected change of mitochondrial degeneration was present. In contrast to colchicine, ivermectin increases microtubule polymerization as with taxol (Ashraf et al, 2015) viz. prevents the disruption of the microtubular network by stabilising it. It is thus not surprising that incubation with ivermectin also resulted in an absence of effect from AG. As a result we believe that this provides sufficient evidence that these abnormal structures seen, are indeed the remnant of a degenerative microtubular network that was first described by Patterson et al (1982).

Further support for this conclusion is found by the accumulation of a substantially larger number of electron-dense and electron-lucent bodies around the degenerative microtubules. In the study by Oliveira et al (2006), the accumulation of granules was linked to damage

micro-tubular network with subsequent inhibition in the movement of secretory granules from sites of synthesis, which would support not only the multivesicular bodies evident in this study and accumulation of secretory bodies. The latter would explain the pitting/erosions in parasite's epicuticle, especially since they are equidistant in their spread. From cuticle physiology from *Caenorhabditis elegans*, it is known that the epicuticle provides a protective envelope to the parasite (Kennedy, 1991, Page and Johnstone, 2007). In addition, the cuticle is impermeable to substances, due to its lipid composition. While the exact physiology of the cuticle's formation and maintenance is unknown at present, it is possible that the erosions are an indication of the epicuticle sloughing from the failure to be replenished. From published literature, electron lucent granules within the parasite are known to contain lipid secretions (Bleve-zacheo, 1993). The damage to the epicuticle also explains the shrunken like appearance of the exposed worms i.e. due to loss of internal content.

Conclusion

Based on the consistent appearance of multi-vesicular bodies following treatment with AG, and the disappearance of pathology in the presence of albendazole a known inhibitor of microtubular polymerisation, AG appears to function through the disruption of the microtubular network.

Acknowledgement

The author would like to thank the staff at the Biomedical Research Centre of the University of Pretoria and the Electron Microscopy staff of the Department of Anatomy and Physiology for providing technical assistance on the project. Many thanks to Prof F Fakoya for his comments on the morulated bodies evident on EM.

Funding

The following project was supported by a grant from the National Research Foundation of South Africa.

Author Contributions

MA: designed the study, isolated agrimol, ran the efficacy assays, data analysis and participated in the preparation of the manuscript; LM: undertook the combination drug assays and participated in data analysis, MDA: assisted with compound identification; ASA: participated in the isolation and elucidation of agrimol; JNE: participated in the study design and manuscript preparation; VN: Obtained funding, participated in the study design, data analysis and manuscript preparation. VN and JNE were degree supervisors of MA.

References

Adamu, M., Naidoo, V. and Eloff, J.N., 2013. Efficacy and toxicity of thirteen plant leaf acetone extracts used in ethnoveterinary medicine in South Africa on egg hatching and larval development of *Haemonchus contortus*. BMC Vet. Res. 9, 38.

Airaksinen, M. M., Mattila, M. J., Takki, S., 1967. The oral toxicity in mice and the uptake by Diphyllobothrium latum and the host gut of some anthelmintics in vitro. Basic Clin. Pharmacol. Toxicol. 25, 33-40.

Aremu, A.O., Fawole, O.A., Chukwujekwu, J.C., Light, M.E., Finnie, J.F., Van Staden, J., 2010. In vitro antimicrobial, anthelmintic and cyclooxygenase-inhibitory activities and phytochemical analysis of *Leucosidea sericea*. J. Ethnopharmacol. 131, 22–27.

Ashraf, S., Beech, R.N., Hancock, M.A., Prichard, R.K., 2015. Ivermectin binds to *Haemonchus contortus* tubulins and promotes stability of microtubules. Int. J. Parasitol. 45,

647-654.

Bleve-zacheo, T., Melillo, M.T., Zacheo, G., 1993. Ultrastructural studies on the nematode *Xiphinema diversicaudatum*: oogenesis and fertilization. Tissue Cell, 25, 375-388.

Bosman, A.A., Combrinck, S., Roux-Van der Merwe, R., Botha, B.M., McCrindle, R.I., Houghton, P.J., 2004. Isolation of an anthelmintic compound from *Leucosidea sericea*. S Afr. J. Bot. 70, 509-511.

Brunet, S., Fourquaux, I., Hoste, H., 2011. Ultrastructural changes in the third-stage, infective larvae of ruminant nematodes treated with sainfoin (*Onobrychis viciifolia*) extract. Parasitol. Int. 60, 419-424.

Coates-Palgrave, K., Drummond, R. B., Moll, E. J., Coates Palgrave, M., 2002. Trees of southern Africa, 3rd ed., Struik, Cape Town.

Cristina, R.T., Dumitrescu, E., Pentea, M.C., Stancu, A.C., Muselin, F., 2014. Albendazole Sensitive vs. Resistant Nematodes–The Mitochondrial Ultra-Structural Changes. J. Fac. Vet. Med. Istanbul Univ. 41, 43-49.

Gerson, T., Shorland, F.B., Dunckley, G.G., 1964. The effect of β-sitosterol on the metabolism of cholesterol and lipids in rats on a diet low in fat. Biochem. J. 92: 385-390.

Gonçalves, J.P., Oliveira-Menezes, A., Junior, A.M., Carvalho, T.M., de Souza, W., 2013. Evaluation of Praziquantel effects on Echinostoma paraensei ultrastructure. Vet. Parasit. 194, 16-25.

Githiori, J.B., Hoglund, J., Waller, P.J., Baker, R.L., 2004. Evaluation of anthelmintic properties of some plants used as livestock dewormers against *Haemonchus contortus* infections in sheep. Vet. Parasit. 129, 245–253.

Hausmann, K., Linnenbach, M., Patterson, D.J., 1983. The effects of taxol on microtubular arrays: in vivo effects on heliozoan axonemes. J. Ultrastruct. R. 82, 212-220.

Hoste, H., Jackson, F., Athanasiadou, S., Thamsborg, S., Hoskin, S.O., 2006. The effects of tannin-rich plants on parasitic nematodes in ruminants. Trends Parasitol. 22, 253–261.

Hutchings, A., Scott, A.H., Lewis, G., Cunningham, A.B., 1996. Zulu Medicinal Plants: An Inventory. University of Natal Press, Pietermaritzburg.

Jasmer, D.P., Yao, C., Rehman, A., Johnson, S., 2000. Multiple lethal effects induced by a benzimidazole anthelmintic in the anterior intestine of the nematode *Haemonchus contortus*. Mol. Biochem. Parasitol. 105, 81-90.

Kennedy, M.W., 1991. Parasitic Nematodes SH Antigens, Membranes & Genes. Taylor and Francis, London.

Köhler, P., 2001. The biochemical basis of anthelmintic action and resistance. Int. J. Parasitol. 31, 336-345.

Lounasmaa, M., Widén, C.J. Huhtikangas, A., 1973. Phloroglucinol derivatives of *Hagenia abyssinica*. Phytochemistry. 12, 2017-2025.

Mehlhorn, H., Harder, A., 1997. Effects of the synergistic action of febantel and pyrantel on the nematode *Heterakis spumosa*: a light and transmission electron microscopy study. Parasitol. Res. 83, 419-434.

Montasser, A.A., Amin, A., 2010. Effect of ivermectin on the integument and dorsoventral muscles of the tick *Argas* (*Persicargas*) *persicus* (Oken)(Ixodoidea: Argasidae). Parasitol. Res. 107, 975-982.

Nair, J.J., Aremu, A.O., Van Staden, J., 2012. Anti-inflammatory effects of *Leucosidea sericea* (Rosaceae) and identification of the active constituents. S. Afr. J Bot. 80, 75-76.

Oliveira, F.A.D., Kusel, J.R., Ribeiro, F. and Coelho, P.M.Z., 2006. Responses of the surface membrane and excretory system of *Schistosoma mansoni* to damage and to treatment with praziquantel and other biomolecules. Parasitol. 132, 321-330.

Page, A.P., Johnstone, I.L., 2007. The cuticle In: The *C. elegans* Research Community WormBook (Ed.), WormBook, http://www.wormbook.org.

Patterson, D.J., Hausmann, K., 1982. Morulate bodies in Actinophryid heliozoa: A fixation artefact derived from microtubules? Cell Struct. Funct. 7, 341-348.

Pooley, E., 1993. The Complete Field Guide to Trees of Natal, Zululand and Transkei. Natal Flora Publications Trust, Durban.

Rothwell, J., Sangster, N., 1997. *Haemonchus contortus*: the uptake and metabolism of closantel. Int. J. Parasitol. 27, 313-319.

Singh, I.P., Bharate, S.B., 2006. Phloroglucinol compounds of natural origin Nat. Prod. Rep. 23, 558–591.

Van Soest, P.J., 1994. Nutritional ecology of the ruminant. Cornell University Press. London.

Van Wyk, J.A., Stenson, M.O., Van der Merwe, J.S., Vorster, R.J., Viljoen, P.G., 1999. Anthelmintic resistance in South Africa: surveys indicate an extremely serious situation in sheep and goat farming. Onderstepoort J. Vet. 66. 273.

Waller, P.J., 2006. From discovering to development. Current industry perspectives for the development of novel methods of helminth control in livestock. Vet. Parasitol. 139, 1-14.

Wang, S., Zhang, Q., Zhang, Y., Shen, C., Wang, Z., Wu, Q., Zhang, Y., Li, S., Qiao, Y., 2016. Agrimol B suppresses adipogenesis through modulation of SIRT1-PPAR gamma signal pathway. Biochem. Bioph. Res. Co. 477, 454-460.

Watt, J.M., Breyer-Brandwijk, M.G., 1962.The Medicinal and Poisonous Plants of Southern and Eastern Africa, 2nd Ed. Livingstone, London.

Yamaki, M., Kashihara, M., Ishiguro, K., Takagi, S., 1989. Antimicrobial Principles of Xian he cao (*Agrimonia pilosa*). Planta med. 55, 169-170.

Zintz, K., Frank, W., 1982. Ultrastructural modifications in *Heterakis spumosa* after treatment with febantel or mebendazole. Vet. Parasitol. 10, 47-56.

Figure 1: Structure of the three isolated compounds β-sitosterol (1), Agrimol G (2) and Agrimol A (3) from *Leucosidea sericea*

Figure 2: Comparative effect of the various treatments against naturally harvested haemonchus adult parasites maintained under ex vivo conditions. The micrographs show severe damage to the cuticle following treatment with agrimol (B), moderate changes from albendazole (D), and a normal cuticle from the saline control (A) and treatment with ivermectin (C)

Figure 3: Transmission electron microscopy with focus on the mitochondria. The treatment with saline (A) showed no mitochondrial changes, while treatment with the crude extract (B) and agrimol (C) show the presence of round non-membranous structures which has a morulated appearance (small white arrow), while treatment with albendazole (D) also showing increased vacuolisation and early changes to the shape of the mitochondria (open white arrow). Also visible are the mitochondria (black arrow) and secretory bodies (large white arrow)

Figure 4: Transmission electron microscopy of the cuticle (Cu) of the parasite in the control group (A) agrimol group (B) and ivermectin group (C). The epi-cuticle (black arrow) shows damage in the agrimol treatment group. The hypodermis (white arrow) in the agrimol group appeared my vacuolated. Also evident is the muscle layer (m). In the ivermectin treatment group, the muscle layers is no longer easily visible.

Figure 5: SEM following co-incubation of agrimol with albendazole (A) or ivermectin (B) (magnification). In the presence of ivermectin and albendazole, agrimol was rendered ineffective. The open arrow shows mitochondrial swelling for the albendazole group.

Figure 6: SEM following co-incubation of agrimol at 1.2, 0.6, 0.3 and 0 mg/mL. The two high exposure concentration show severe generalised cuticle damage, while the 0.3 mg/ml shows more localised damage (arrow).

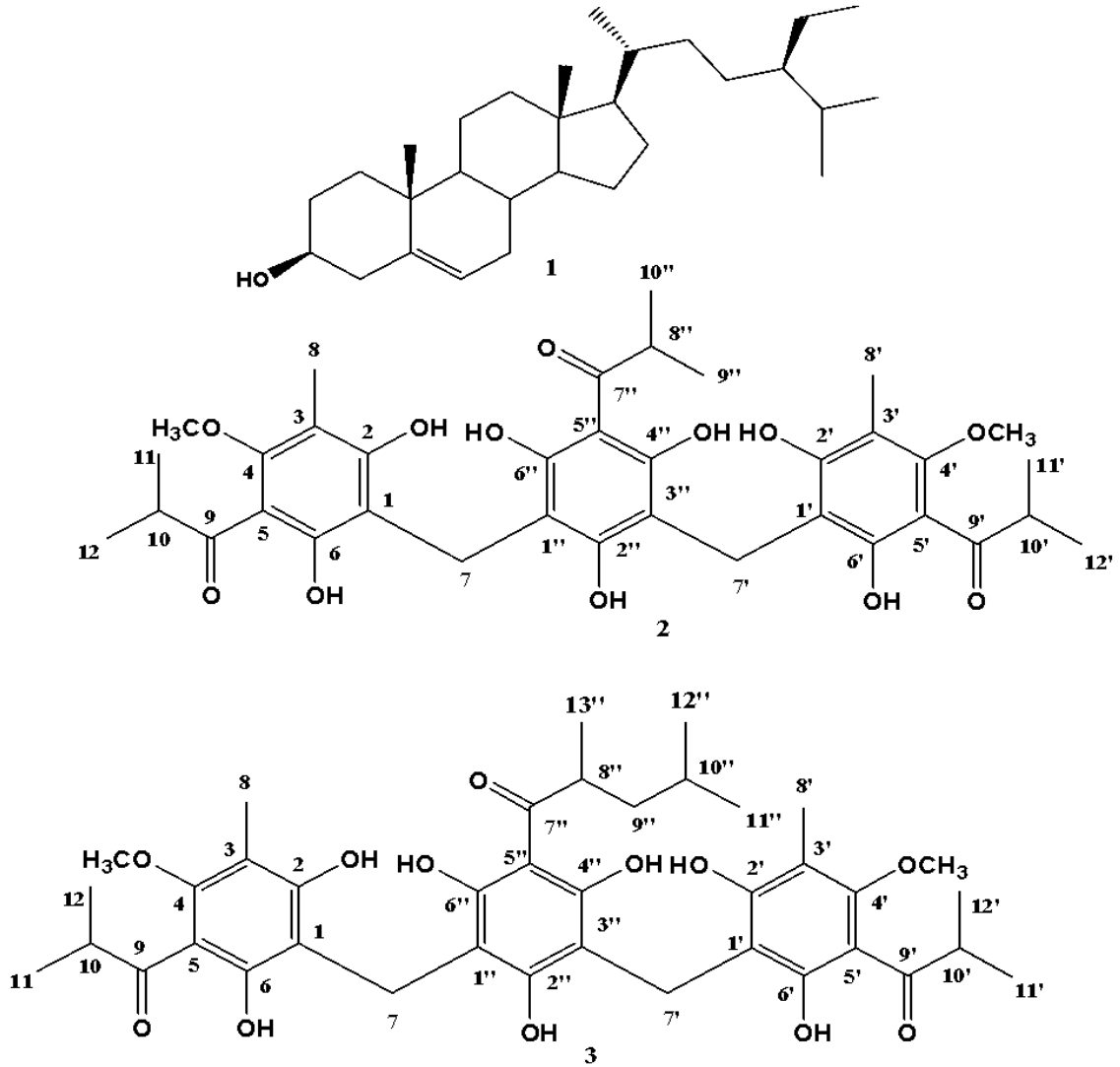
HO
1
10''
8''
9''
7''
O
8
3
2
OH
H3CO
11
4
1
9
5
6
12
10
O
OH
7
HO
5''
4''
OH
6''
3''
1''
2''
OH
7'
HO
2'
3'
8'
OCH3
4'
11'
1'
9'
5'
6'
10'
12'
OH
O
2
13''
12''
8''
10''
11''
7''
9''
O
8
3
2
OH
H3CO
12
4
1
9
5
6
10
11
O
OH
7
HO
5''
4''
OH
6''
3''
1''
2''
OH
7'
HO
2'
3'
8'
OCH3
4'
12'
1'
9'
5'
6'
10'
11'
OH
O
3

Figure 1

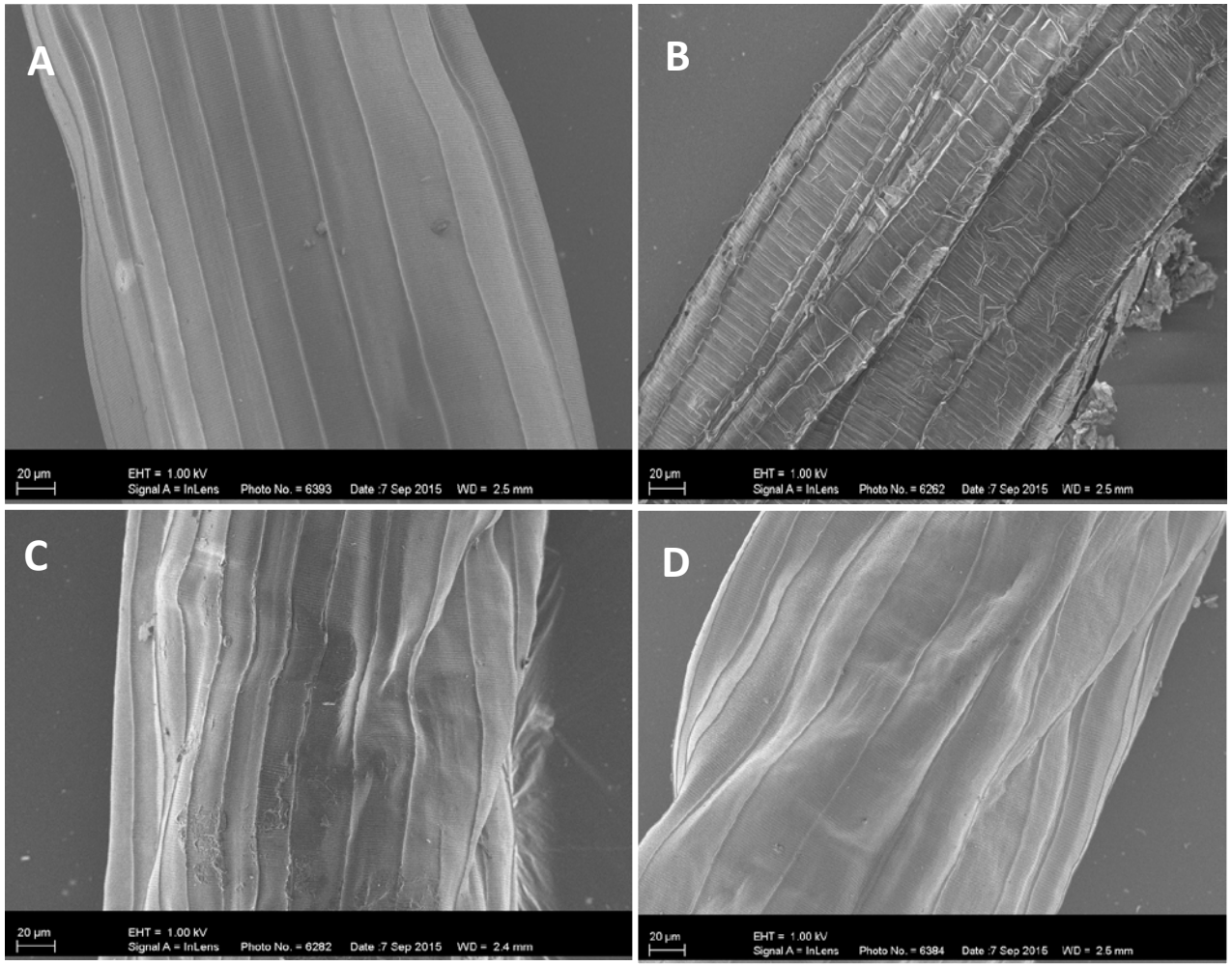
A
20 µm
EHT = 1.00 kV
Signal A = InLens
Photo No. = 6393
Date :7 Sep 2015
WD = 2.5 mm
B
20 µm
EHT = 1.00 kV
Signal A = InLens
Photo No. = 6262
Date :7 Sep 2015
WD = 2.5 mm
C
20 µm
EHT = 1.00 kV
Signal A = InLens
Photo No. = 6282
Date :7 Sep 2015
WD = 2.4 mm
D
20 µm
EHT = 1.00 kV
Signal A = InLens
Photo No. = 6384
Date :7 Sep 2015
WD = 2.5 mm

Figure 2

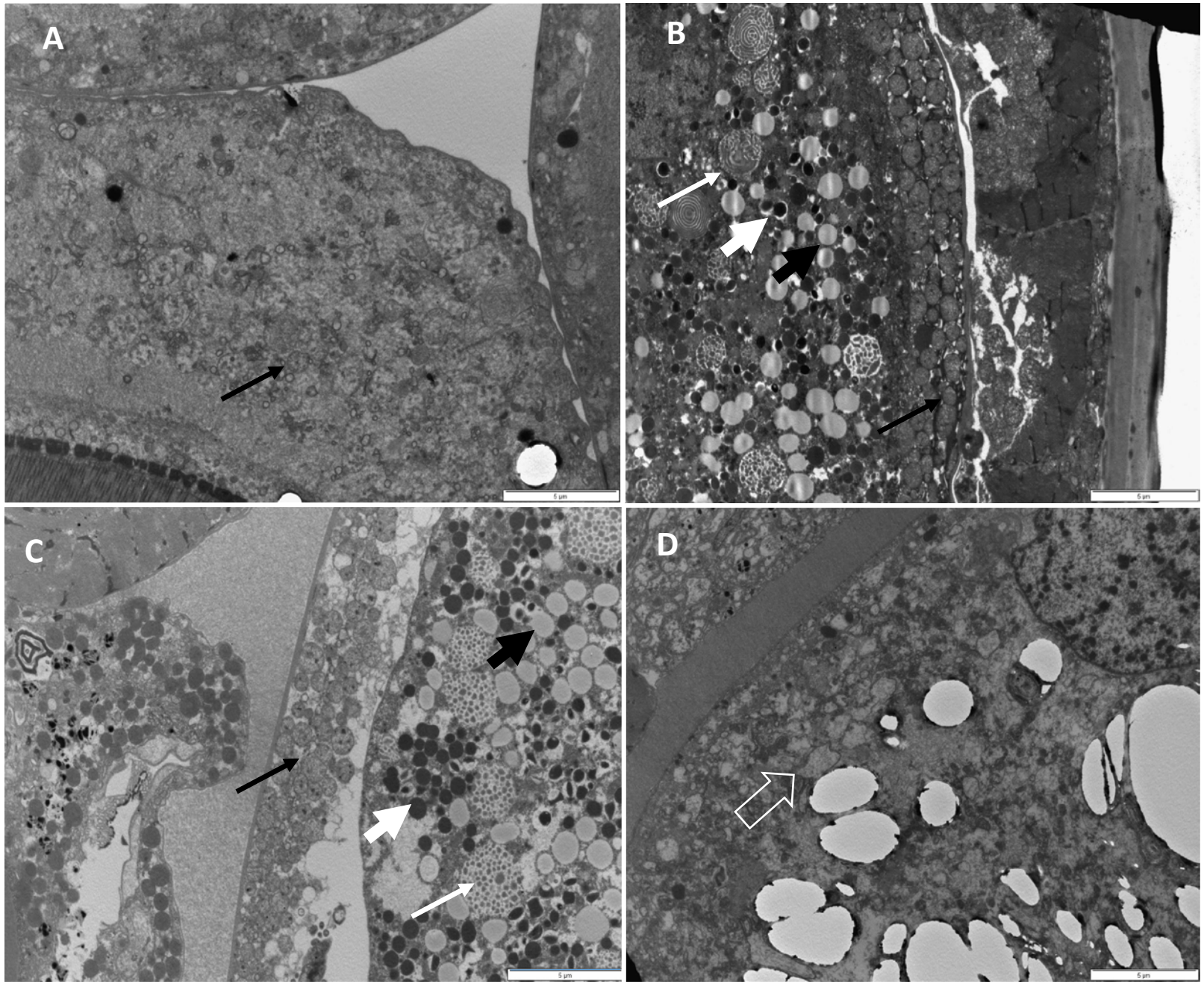

Figure 3

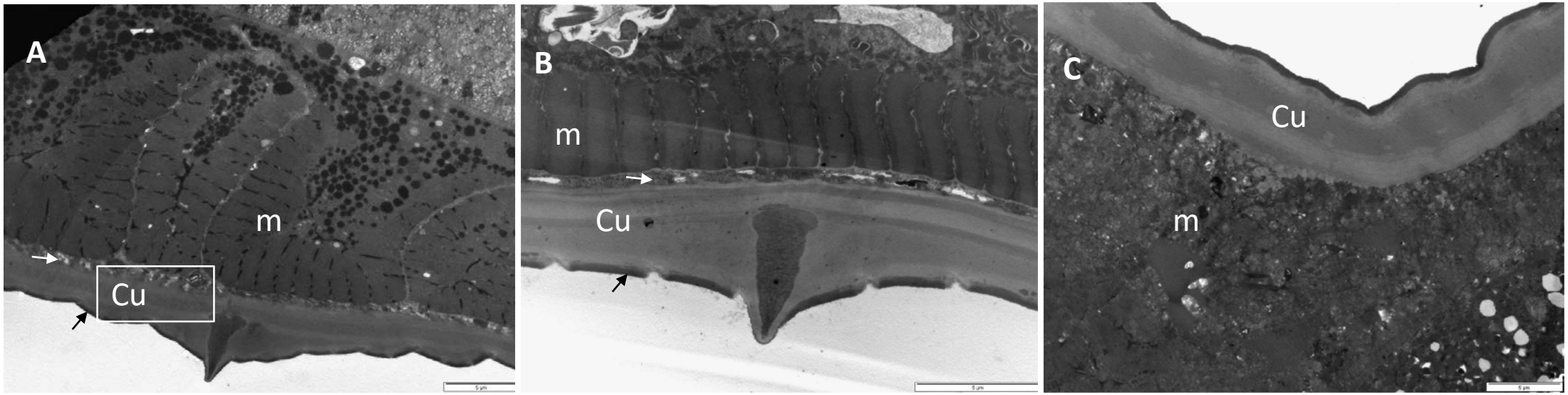

Figure 4

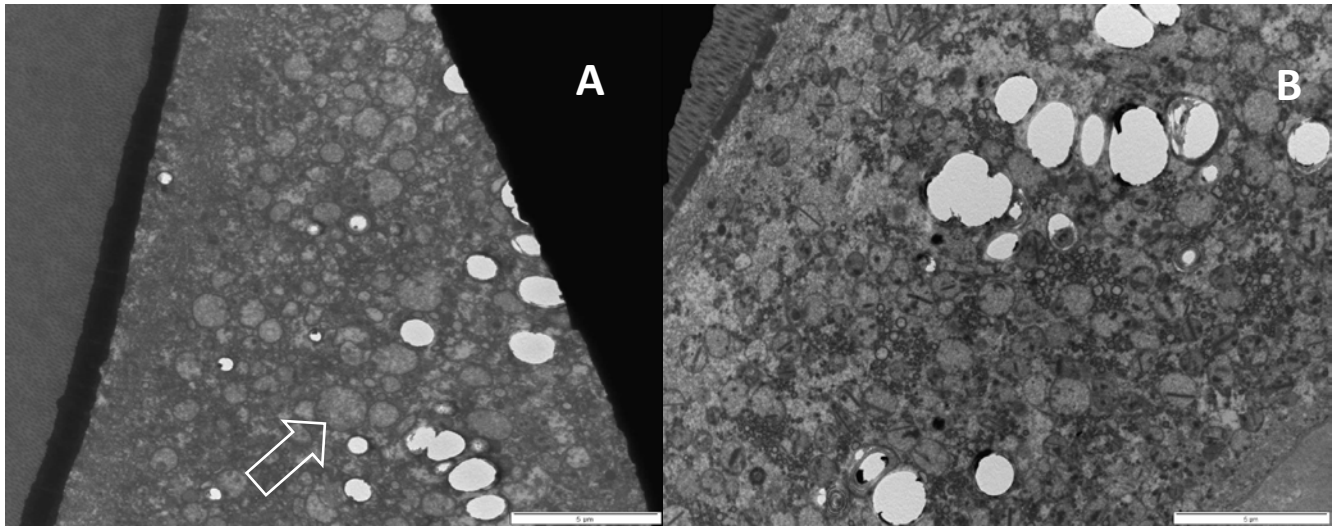

Figure 5

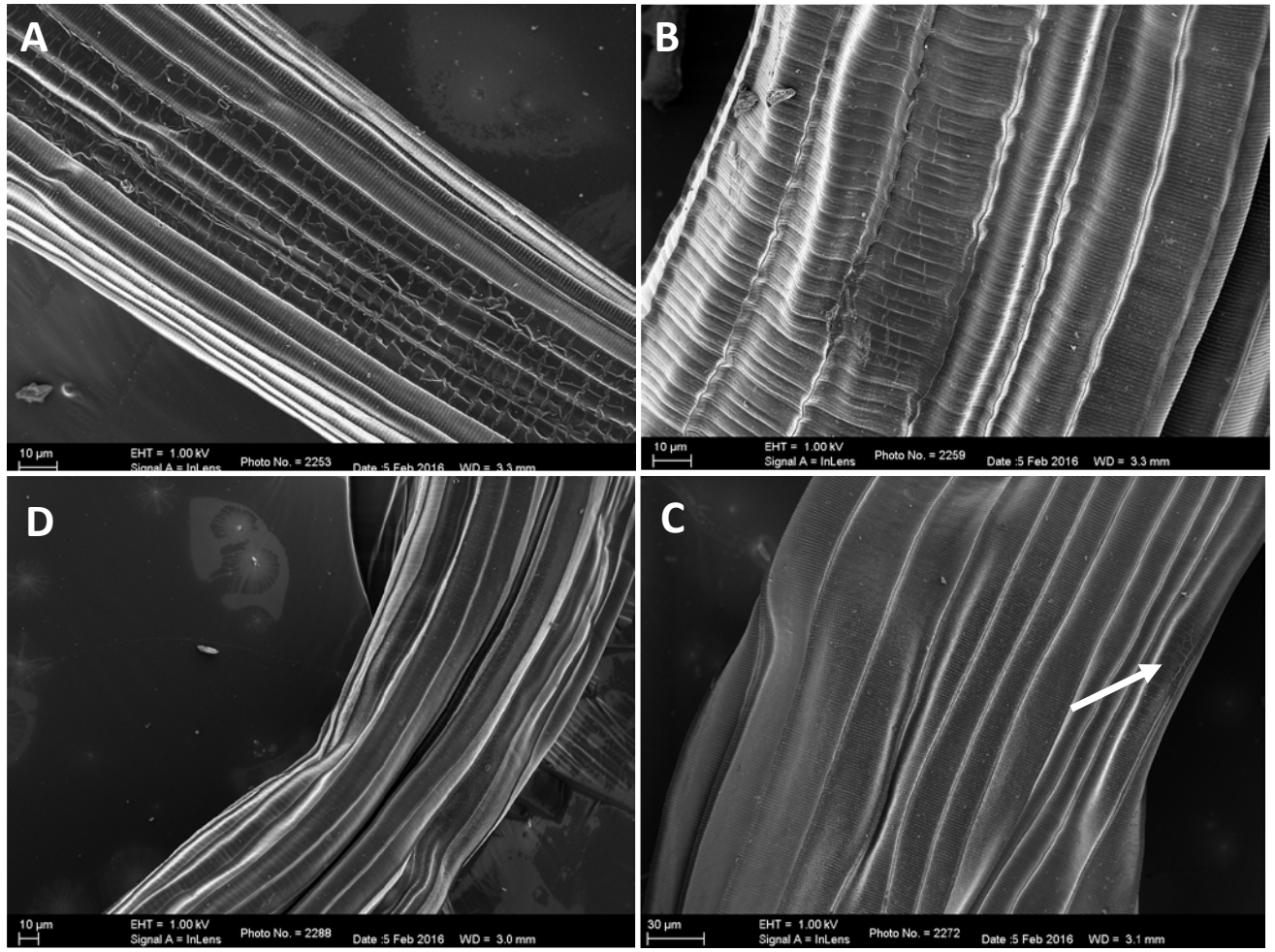
A
10 µm
EHT = 1.00 kV
Signal A = InLens
Photo No. = 2253
Date :5 Feb 2016
WD = 3.3 mm
B
10 µm
EHT = 1.00 kV
Signal A = InLens
Photo No. = 2259
Date :5 Feb 2016
WD = 3.3 mm
D
10 µm
EHT = 1.00 kV
Signal A = InLens
Photo No. = 2288
Date :5 Feb 2016
WD = 3.0 mm
C
30 µm
EHT = 1.00 kV
Signal A = InLens
Photo No. = 2272
Date :5 Feb 2016
WD = 3.1 mm

Figure 6

Supplementary Material

Infrared information for the two isolation Agrimol Molecules.

Agrimol A

Amorphous yellow powder; IR ν_{max}: 3400-3150, 2914, 1610, 1269, 1150, 1100, 984, 652 cm^{-1}; ^{13}C-NMR data ($CDCl_3$, 125 MHz) δ: 212.5 (C-9/C-9'), 204.2 (C-7''), 160.4 (C-2''/C-4/C-4'/C-6/C-6'), 159.7 (C-2/C-2'/C-4''/C-6''), 109.4 (C-1/C-1'/C-1''/C-3''), 108.0 (C-3/C-3'), 105.7 (C-5/C-5'/C-5''), 61.4 (4-OCH_3/4'-OCH_3), 52.9 (C-9''), 46.0 (C-8''), 38.3 (C-10/C-10'), 36.6 (C-10''), 24.9 (C-13''), 22.7 (C-11/C-11'/C-12/C-12'), 19.2 (C-11''/C-12''), 16.6 (C-7'), 16.4 (C-7), 9.1 (C-8/C-8').

Agrimol G

The compound was an amorphous yellowish powder; IR ν_{max}: 3400-3100, 2934, 1610, 1269, 1154, 1106, 984, 652 cm^{-1}; ^{1}H-NMR ($CDCl_3$, 500 MHz) δ 1.15 (4H, d, J = 8.5 Hz, H-11/H-12/H-11'/H-12'), 1.19 (2H, d, J = 8.4 Hz, H-9''/H-10''), 2.12 (2H, s, H-8/H-8'), 3.70 (6H, s, 4-OMe/4'-OMe), 3.82 (4H, s, H-7/H-7'), 3.86 (2H, m, H-10/H-10'), 4.02 (1H, m, H-8''), 9.22 (br s, 2''-OH), 9.60 (br s, 2'-OH), 9.70 (br s, 6-OH), 10.70 (br s, 2-OH), 15.50 (br s, 6''-OH), 15.87 (br s, 6'-OH), 16.07 (br s, 4''-OH); ^{13}C-NMR data ($CDCl_3$, 125 MHz) δ: 212.5 (C-9/C-9'), 211.8 (C-7''), 160.0 (C-2''/C-4/C-4'/C-6/C-6'), 157.9 (C-2/C-2'/C-4''/C-6''), 106.6 (C-1/C-1'/C-1''/C-3''), 105.8 (C-3/C-3'), 104.8 (C-5/C-5'/C-5''), 62.1 (4'-OCH_3), 39.3 (C-8''), 38.3 (C-10/C-10'), 19.8 (C-9''/C-10''), 19.3 (C-11/C-11'/C-12/C-12'), 16.9 (C-7'), 16.5 (C-7), 9.2 (C-8/C-8').